

## INVERSE DETERMINATION OF SPATIALLY VARYING HEAT CAPACITY AND THERMAL CONDUCTIVITY IN ARBITRARY 2D OBJECTS

Sohail R. Reddy, George S. Dulikravich and S. M. Javad Zeidi

\*Department of Mechanical and Materials Engineering, MAIDROC Laboratory

Florida International University, Miami, Florida, USA

Email: sredd001@fiu.edu, dulikrav@fiu.edu, szeit001@fiu.edu

**ABSTRACT** A methodology for non-destructive simultaneous estimation of spatially varying thermal conductivity and heat capacity in 2D solid objects was developed that requires only boundary measurements of temperatures. The spatial distributions were determined by minimizing the normalized sum of the least-squares differences between measured and calculated values of the boundary temperatures. Computing time was significantly reduced for the entire inverse parameter identification process by utilizing a metamodel created by an analytical response surface supported by an affordable number of numerical solutions of the temperature fields obtained by the high fidelity finite element analyses. The minimization was performed using a combination of particle swarm optimization and the BFGS algorithm. The methodology has shown to accurately predict linear and nonlinear spatial distributions of thermal conductivity and heat capacity in arbitrarily shaped multiply-connected 2D objects even in situations with noisy measurement data thus proving that it is robust and accurate. The current drawback of this method is that it requires an a priori knowledge of the general spatial analytic variation of the physical properties. This can be remedied by representing such variations using products of infinite series such as Fourier or Chebyshev and determining correct values of their coefficients.

### INTRODUCTION

With advances in rapid prototyping, it is now possible to create solid objects with spatially varying material properties. It becomes then imperative to determine the spatial distribution of these properties that will create desired responses of the objects. This paper deals with an inverse approach for simultaneous non-destructive determination of spatially varying material properties. This method does not require any information from within a solid object and therefore it is non-invasive.

Electrical and thermal properties such as electric permittivity, magnetic permeability, thermal capacity and thermal conductivity influence the spatial variation of the field variable,  $\phi = \phi(x, y)$  such as electric, magnetic and temperature fields. Steady field problems of this type can be modelled by an elliptic partial differential equation governing the steady-state diffusion of  $\phi$ .

$$\nabla \cdot (\lambda \phi) = 0 \quad (1)$$

Here,  $\lambda = \lambda(x, y)$  is the diffusion coefficient (physical property of the media). Having a mathematical model, the question to answer becomes: *Using only boundary values of the field variable  $\phi$ , or its normal derivatives on the boundary of the solid, how can the spatial distribution of the physical property,  $\lambda$ , be determined throughout the arbitrarily shaped object?*

In the forward problem, the solution of Eq. (1) can easily be obtained either analytically, or numerically through finite element or finite volume integration for a known distribution of  $\lambda$ . In an inverse problem,  $\lambda$  is not known and must be determined non-destructively. This typically requires the values of the field variable  $\phi$  and its normal derivatives to be known on the boundary. Since most of the solution methods [1-7] of such ill-posed problems are iterative, they require regularization.

This inverse problem is somewhat more tractable if the diffusion coefficient  $\lambda$  is assumed to vary as a function of  $x, y, z$  coordinates according to some analytic functions defined by a number of unknown parameters and the coordinates  $x, y, z$ . The inverse problem can then be solved by minimizing the scaled sum of squared differences between the computed  $\phi$  or  $\partial\phi/\partial n$  values on the boundaries obtained from the assumed distribution of material properties and the measured  $\phi$  or  $\partial\phi/\partial n$  on the boundaries. In this approach, the initial distribution of material properties is assumed and iteratively updated (by varying the values of the parameters) until the scaled sum of squares of differences is below a specific threshold. This inverse parameter identification concept was previously used to estimate a single spatially varying material property [8-10] based on solutions of steady state equation (1). It is here extended to simultaneously determining two spatially varying material properties: heat capacity and thermal conductivity. Both linear and non-linear distributions of these two properties were non-destructively simultaneously estimated in 2D solid objects.

## MATHEMATICAL MODELS AND VERIFICATION OF SOFTWARE ACCURACY

The transient heat conduction problem is discretized using the finite element method. The governing equation for transient heat conduction with spatially varying material properties can be written as

$$\rho C_p \frac{\partial T}{\partial t} = \nabla \cdot (k \nabla T) \quad (2)$$

Here,  $\rho$  is density,  $C_p$  is heat capacity,  $T$  is temperature,  $t$  is time, and  $k$  is thermal conductivity. This is done by multiplying Eq. (2) with a test function,  $v$ , and integrating over the domain,  $\Omega$ . The resulting equation becomes

$$\int_{\Omega} \rho C_p \frac{\partial T}{\partial t} v \, d\Omega = \int_{\Omega} \nabla \cdot (k \nabla T) v \, d\Omega \quad (3)$$

The right hand term can be expanded using divergence theorem and the equation can be rewritten as

$$\int_{\Omega} \rho C_p \frac{\partial T}{\partial t} v \, d\Omega = \int_{\partial\Omega} v k \nabla T \cdot \hat{n} \, dS - \int_{\Omega} \nabla v \cdot (k \nabla T) \, d\Omega \quad (4)$$

Here,  $S$  is the surface of the control volume,  $\Omega$ , while  $v$  is the test function. Representing the temperature and test function as a linear combination of finite element basis functions such that

$$T = \sum_{i=1}^{i_{max}} \alpha_i \phi_i \quad (5)$$

yields

$$[C]\{\dot{T}\} + [K]\{T\} = \{R_q\} \quad (6)$$

Here,

$$C_{ji} = \int_{\Omega} \rho C_p \phi_j v d\Omega \quad (7)$$

$$K_{ij} = \int_{\Omega} \nabla v_i \cdot (k \nabla \phi_j) d\Omega \quad (8)$$

$$R_{q,j} = \int_{\partial\Omega} q_s v_j dS \quad (9)$$

where  $q_s$  is the boundary heat flux. The test functions become zero at the boundary nodes where Dirichlet condition is specified leading to the first term on the right side of Eq. (4) equalling to zero. It should be noted that convection, radiation and internal heat sources/sinks were neglected in this derivation.

The finite element solver was validated against an analytical solution for a 2D, steady-state heat conduction problem with spatially varying thermal conductivity on a square domain. Consider an arbitrary 2D domain with the distribution of thermal conductivity given as

$$k(x, y) = (A + x)(B + y) \quad (10)$$

where A and B are arbitrary constants. Then the analytical temperature field that satisfies the steady-state form of Eq. (2) takes the general form

$$T(x, y) = (A + x)^2 - (B + y)^2 + 273 \quad (11)$$

Figure 1 shows the analytical and numerical solutions to the steady-state heat conduction equation on a square with  $x, y \in [0, 2]$ , subject to boundary conditions given by Eq. (11) where  $A = B = 1.0$ . It can be observed that the numerical method produces accurate solution.

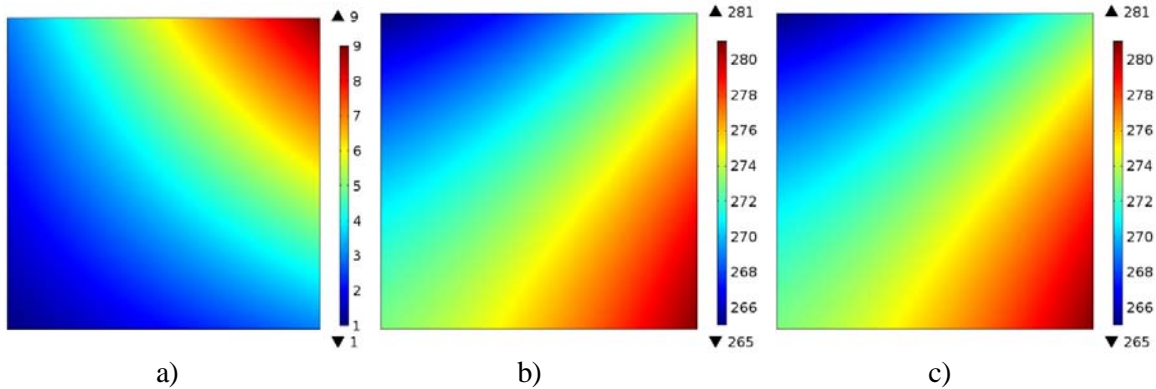


Figure 1. Verification of software accuracy for spatial distribution of: a) thermal conductivity given by Eq. (8), b) analytical temperature given by Eq. (9) and c) temperature calculated by COMSOL

## INVERSE PARAMETER IDENTIFICATION METHODOLOGY

Spatially varying material properties can be determined from over-specified thermal boundary conditions using a variety of iterative algorithm including Bayesian statistics employing Kalman filter or non-linear filters [11]. The methodology presented herein uses a more versatile and computationally

efficient approach based on a combination of a field analysis algorithm (using finite volume, finite elements, *etc.*) and an accurate and robust minimization algorithm capable of avoiding local minima.

The methodology utilized in this work, minimizes the normalized least-squares difference between measured and calculated values of the field variable by iteratively adjusting these parameters. Let us refer to the temperature or temperature gradient on the boundaries obtained from experiments or analytical solution as “measured” values. Let us refer to temperature or temperature gradient on the boundaries obtained from the solution of the forward problem with guessed values of the parameters defining the spatial distribution of thermal conductivity and heat capacity as “calculated” values. Then the functional to minimize becomes

$$J = \sum_{m=1}^{mmax} \sum_{\partial\Omega} \left[ \frac{T_{calc.}^m - T_{meas.}^m}{T_{meas.}^m + \varepsilon} \right]^2 \quad (12)$$

where  $\varepsilon$  is a very small positive number of the order 1.0E-06 and the summation is performed over the boundary of the arbitrarily shaped domain, and over  $mmax$  number of time steps. The  $J$  functional is minimum when the thermal conductivity and heat capacity, from which the “calculated” and “measured” are obtained, are the same.

The minimization of Eq. (12) was performed using a hybrid of evolutionary particle swarm and Broyden-Fletcher-Goldfarb-Shanno (BFGS) gradient-based optimization algorithms [12, 13]. Given  $\mathbf{x}_0$  and an approximate Hessian matrix  $B_0$ , the BFGS algorithm progresses as follows.

- 1) Evaluate the search direction  $\mathbf{p}_k$  by solving  $B_k \mathbf{p}_k = -\nabla f(\mathbf{x}_k)$
- 2) Update  $\mathbf{x}_{k+1} = \mathbf{x}_k + \alpha_k \mathbf{p}_k$  where  $\alpha_k$  is an acceptable step size found using line search
- 3) Set  $\mathbf{s}_k = \alpha_k \mathbf{p}_k$
- 4)  $\mathbf{y}_k = \nabla f(\mathbf{x}_{k+1}) - \nabla f(\mathbf{x}_k)$
- 5)  $B_{k+1} = B_k + \frac{\mathbf{y}_k \mathbf{y}_k^T}{\mathbf{y}_k^T \mathbf{s}_k} - \frac{B_k \mathbf{s}_k \mathbf{s}_k^T B_k}{\mathbf{s}_k^T B_k \mathbf{s}_k}$

The optimizer iteratively modifies the parameters in the analytic expressions for thermal conductivity and heat capacity in the forward (analysis) problem during minimization of the  $J$  functional. In several cases, the solution of forward problem can be very computationally expensive. In most inverse problems dealing with parameter identification, the forward problem needs to be solved a large number of times, each time for different guessed values of parameters in material properties, until the methodology converges. For this reason, it is very appealing to replace the finite element solver with a slightly less accurate but much faster surrogate model. The surrogate model used in this work is a response surface for the  $J$  functional, based on Radial Basis Functions [13]. The response surface of the  $J$  functional was created by interpolating  $J$  values calculated using COMSOL. The interpolation points were uniformly distributed throughout the search space using Sobol’s algorithm [14]. Figure 2 shows the workflow of the complete inverse problem methodology implemented. First, the response surface is constructed using values obtained from COMSOL. The constructed surrogate model was then coupled with the hybrid optimizer to minimize the  $J$  functional.

All computations were performed on a single thread of Intel Xeon CPU E5-4620v2@2.60 GHz with 256GB of RAM. Each transient COMSOL solution of equation (2) took approximately 15 seconds. The same non-structured computational grid of 30000 triangular elements was used for each analysis.

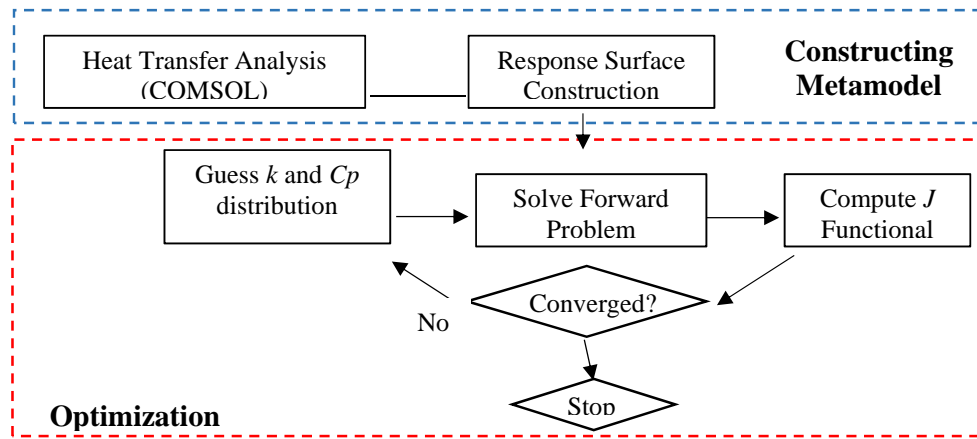


Figure 2. Flow chart of the inverse problem methodology

### NUMERICAL RESULTS FOR ARBITRARY 2D GEOMETRY

The proposed inverse problem methodology was validated for several cases considering linear and non-linear spatial distribution of material properties in an arbitrary geometry. Table 1 shows the equations defining the arbitrary multiply-connected 2D geometry shown in Fig. 3.

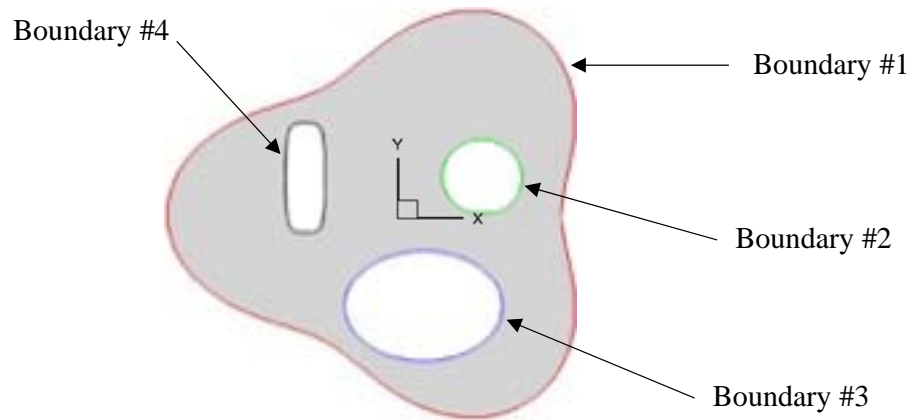


Figure 3. Arbitrary configurations defined using equations in Table 1.

Table 2 shows the thermal boundary conditions applied to each of the four boundaries. The boundary conditions were kept the same for each case. All heat fluxes in this work are considered to be inwards and normal to the surface.

Table 1  
Geometry definition of arbitrary multiply-connected solid considered in this work

	Equation	# Cells on Boundary
Boundary 1	$r = r_0 - A \cos(3\theta)$ , where $r_0 = 1, A = 0.2, 0.0 \leq \theta \leq 2\pi$	250
Boundary 2	$\left[ \frac{x-0.4}{0.2} \right]^2 + \left[ \frac{y-0.2}{0.2} \right]^2 = 1$	198
Boundary 3	$\left[ \frac{x-0.1}{0.4} \right]^2 + \left[ \frac{y+0.5}{0.3} \right]^2 = 1$	346
Boundary 4	$\left[ \frac{x+0.5}{0.1} \right]^4 + \left[ \frac{y-0.2}{0.3} \right]^4 = 1$	213

Table 2  
Thermal boundary conditions applied to the arbitrary geometry

Boundary conditions	
Boundary #1	$T = 353 \text{ K}$
Boundary #2	$q = 100 * k(x,y)$
Boundary #3	$q = 50 * k(x,y)$
Boundary #4	$q = 125 * k(x,y)$

**Case 1: Estimation of Bilinear Distribution of  $C_p$  and  $k$  in Arbitrary 2D Objects**

Ability of this methodology was first tested assuming bilinear variations of thermal conductivity and heat capacity given by Eq. (13) and Eq. (14), respectively. This means that the optimizer needs to find values of four parameters that minimizes the  $J$  functional.

$$k(x, y) = (A_k + x)(B_k + y) \tag{13}$$

$$C_p(x, y) = (A_{C_p} + x)(B_{C_p} + y) \tag{14}$$

The response surface for this test case was constructed using 40 COMSOL analyses solutions. The response surface was then coupled with the optimizer. Table 3 shows the exact parameters and converged values of the parameters that define the thermal conductivity and heat capacity distributions in Case 1.

Table 3  
Case 1: Search ranges for each of the four parameters, exact and converged values of the parameters defining thermal conductivity and heat capacity (when  $m_{max} = 10$ )

	$A_k$	$B_k$	$A_{C_p}$	$B_{C_p}$
Min	0.0	0.0	0.0	0.0
Max	20.0	20.0	2.0	2.0
Exact	0.6	1.5	0.04	0.06
Estimated	0.6	1.5	0.04	0.06

It can be seen from Table 3 and Fig. 4 that the optimizer was able to converge to the exact values of the four parameters, thereby accurately determining the two material properties.

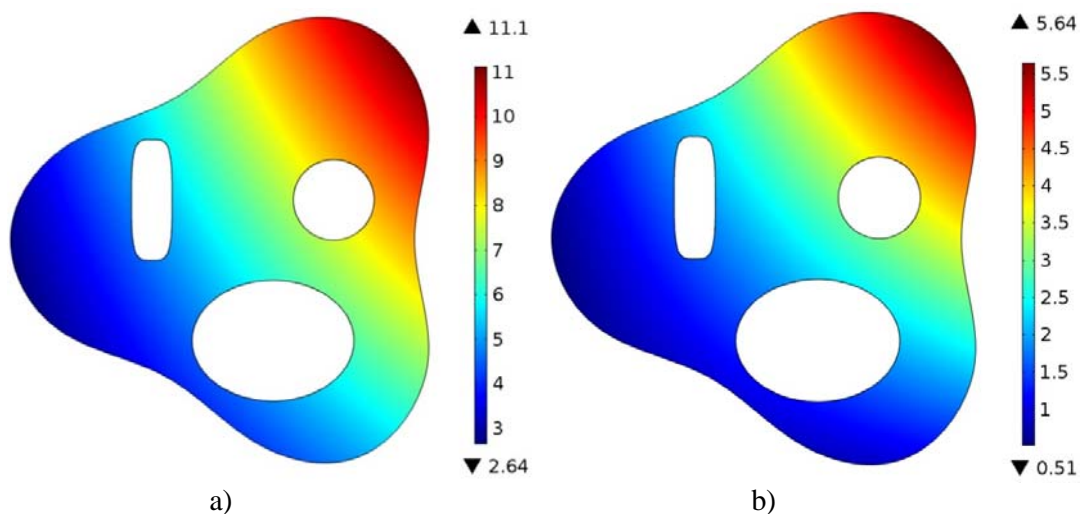


Figure 4. Case 1: Inversely determined distribution of: a) thermal conductivity, and b) heat capacity

### Case 2: Estimation of Nonlinear Distribution of $C_p$ and $k$ in Arbitrary 2D Objects

The proposed methodology was validated for linear distribution of material properties. It is now tested for highly non-linear distributions of material properties. Thermal conductivity and heat capacity were defined the Matyas [15], Eq. (15), and McCormick [15], Eq. (16) functions, respectively. Therefore, a total of six parameters needed to be identified that minimize the  $J$  functional.

$$k(x, y) = A_k(x^2 + y^2) - B_k xy \quad (15)$$

$$C_p(x, y) = \sin(A_{C_p}(x + y)) + B_{C_p}(x - y)^2 - C_{C_p}x + D_{C_p}y + 1 \quad (16)$$

The response surface for this test case was constructed using 60 COMSOL analyses solutions. That is, the heat conduction equation was solved 60 times, each time with different random guesses for the six parameters. Using these 60 calculated values of the  $J$  functional, a six-dimensional response surface was generated using an optimal polynomial radial basis function formulation [13]. Table 4 below shows the exact and the optimizer converged values of the six parameters. It can be seen that even for a non-linear spatial distribution of thermal conductivity and heat capacity, this inverse parameter identification methodology was able to converge to the exact values of the six parameters.

Table 4

Case 2: Search ranges for each of the five parameters, exact and converged values of the parameters defining thermal conductivity and heat capacity (when  $m_{max} = 10$ )

	$A_k$	$B_k$	$A_{C_p}$	$B_{C_p}$	$C_{C_p}$	$D_{C_p}$
Min	0.0	-50.0	0.0	0.0	-2.0	0.0
Max	20.0	-10.0	2.0	2.0	0.0	2.0
Exact	13.6	-43.2	0.3	0.112	-0.012	0.021
Estimated	13.6	-43.2	0.3	0.112	-0.012	0.021

Figure 5 shows the nonlinear distribution of thermal conductivity and heat capacity in Case 2.

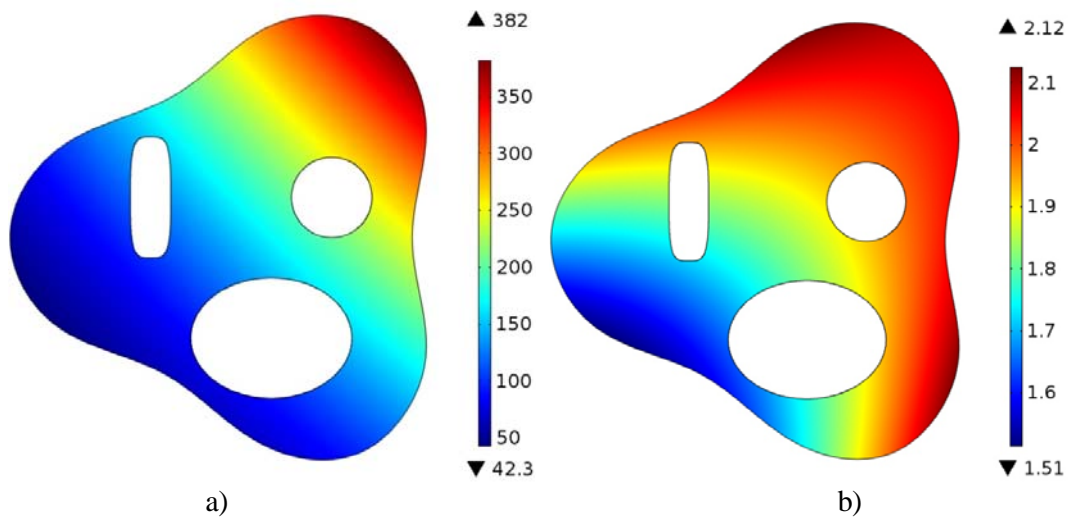


Figure 5. Case 2: Inversely determined distribution of: a) thermal conductivity, and b) heat capacity

### Case 3: Estimation of Nonlinear Distribution of $C_p$ and $k$ with Noisy Measurements

In the previous sections, the proposed methodology was validated for linear and nonlinear distribution of material properties. The “measured” data, in the previous cases, was synthesized using COMSOL software. This does not accurately model the real-life phenomenon. The “measured” data is usually obtained through experimentation and therefore contains some noise. To accurately model such

stochastic behaviour, noise must be added to the synthetic “measured” data obtained using COMSOL. This was done by employing the white Gaussian noise model to add noise [16], of varying intensity, to the “measured” data.

In Case 3, the distribution of thermal conductivity was assumed to follow the generalized Three-Hump Camel Function, Eq. (17), while heat capacity was again assumed to follow the generalized McCormick function, Eq. (18). Therefore, the optimizer needed to find values of the nine parameters that minimize the  $J$  functional. The “measured” boundary temperature values were stochastically perturbed by a noise-to-signal ratio of 1%, 2% and 3%. In reality, the actual Type J, K, E, and T thermocouples and resistance temperature detectors (RTDs) all have a maximum error of approximately 1% [17].

$$k(x, y) = A_k x^2 - B_k x^4 + C_k x^6 + D_k xy + E_k y^2 \quad (17)$$

$$C_p(x, y) = \sin(A_{C_p}(x + y)) + B_{C_p}(x - y)^2 - C_{C_p}x + D_{C_p}y + 1 \quad (18)$$

Table 5

Case 3: Search ranges for each of the nine parameters, exact values, and converged values of the parameters defining the thermal conductivity and heat capacity for various specified noise levels in the “measurements” of boundary temperatures (when  $m_{max} = 10$ )

	$A_k$	$B_k$	$C_k$	$D_k$	$E_k$	$A_{C_p}$	$B_{C_p}$	$C_{C_p}$	$D_{C_p}$
Min	0.0	-5.0	0.0	0.0	0.0	0.0	0.0	-2.0	0.0
Max	20.0	0.0	5.0	20.0	20.0	2.0	2.0	0.0	2.0
Exact	2.0	-1.05	0.1667	1.00	1.00	0.30	0.112	-0.012	0.021
Estimated (0% Error)	2.0	-1.05	0.1667	1.00	1.00	0.30	0.112	-0.012	0.021
Estimated (1% Error)	2.0	-1.04	0.1668	0.99	0.99	0.30	0.112	-0.012	0.021
Estimated (2% Error)	2.0	-1.04	0.1668	1.00	1.00	0.30	0.112	-0.012	0.021
Estimated (3% Error)	2.0	-1.03	0.175	0.93	1.01	0.30	0.109	-0.030	0.027

The nine-dimensional response surface was generated using 90 COMSOL analyses solutions. Because the objective function space was highly nonlinear due to the noisy “measurements”, a more robust hybrid optimizer [18, 19] with an automatic switching among constituent algorithms was used to minimize  $J$  functional. Table 5 shows the exact values and converged calculated values of the nine parameters for various levels of measurement errors. It can be seen that when the noise increases, the optimizer is still able to converge to correct parameters. This is especially promising as most techniques for acquiring thermal measurements have a maximum error of 1%.

Figures 6 and 7 show the distribution of thermal conductivity and heat capacity respectively in Case 3. It can be seen that even for higher values of boundary temperature measurement noise levels, the material properties were predicted accurately using this inverse parameter estimation methodology.

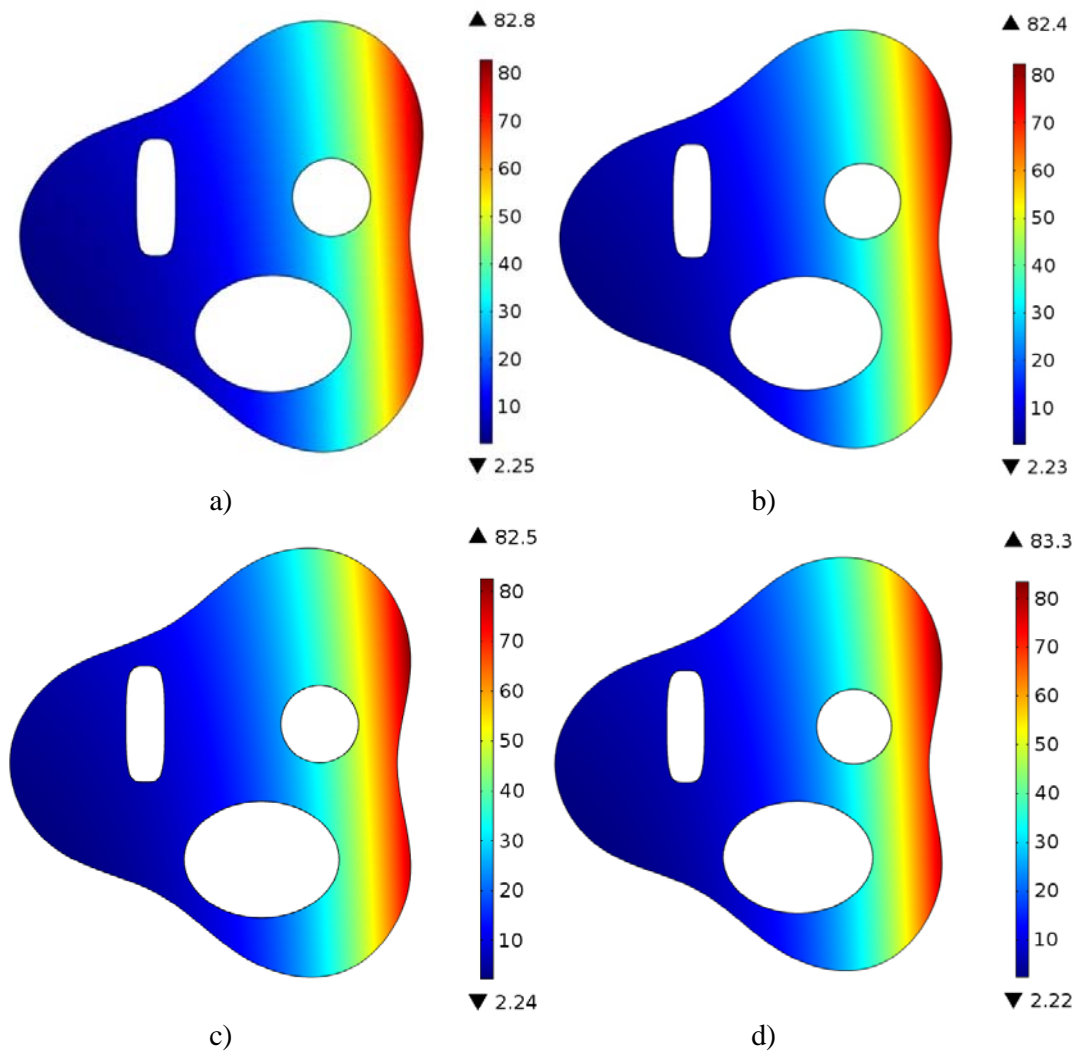


Figure 6. Case 3: Inversely determined distribution of thermal conductivity obtained for boundary temperature measurement noise level of: a) 0%, b) 1%, c) 2% and d) 3%

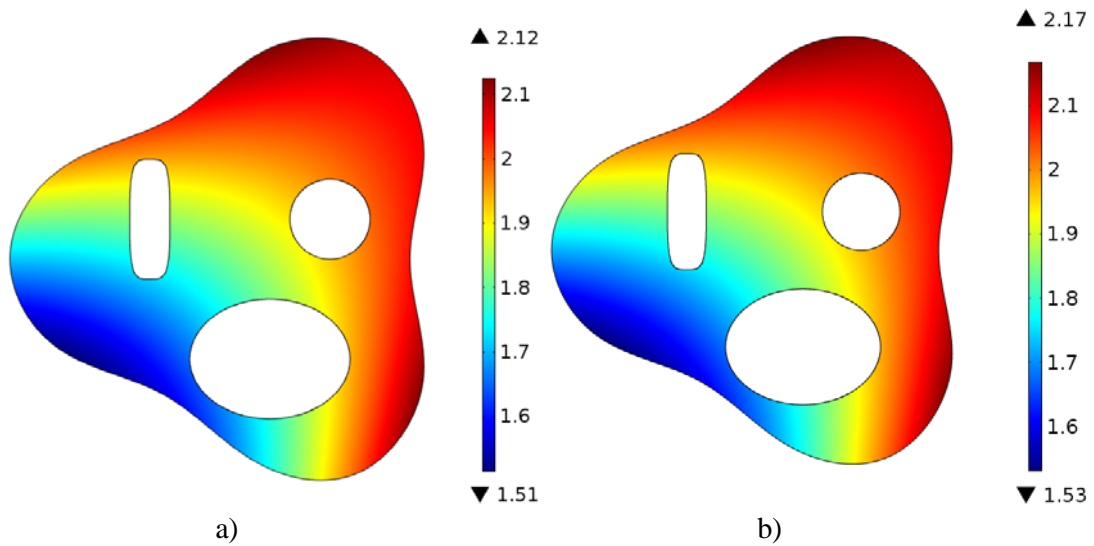


Figure 7. Case 3: Inversely determined distribution of specific heat obtained for boundary temperature measurement noise levels of: a) 0%, 1% and 2%, and b) 3%

Figure 8 shows the relative error distributions for thermal conductivity and heat capacity between their exact and converged values. It can be seen that the maximum local relative error is less than one percent even for large errors in the “measured” boundary values of temperature, confirming that this inverse parameter identification method is robust and accurate.

The key factors contributing to this successful methodology are the use of a highly robust and accurate hybrid optimization algorithm [18, 19], use of a highly accurate multi-dimensional response surface [13], and the fact that we used an *a priori* assumed general analytical spatial variation of thermal conductivity and heat capacity.

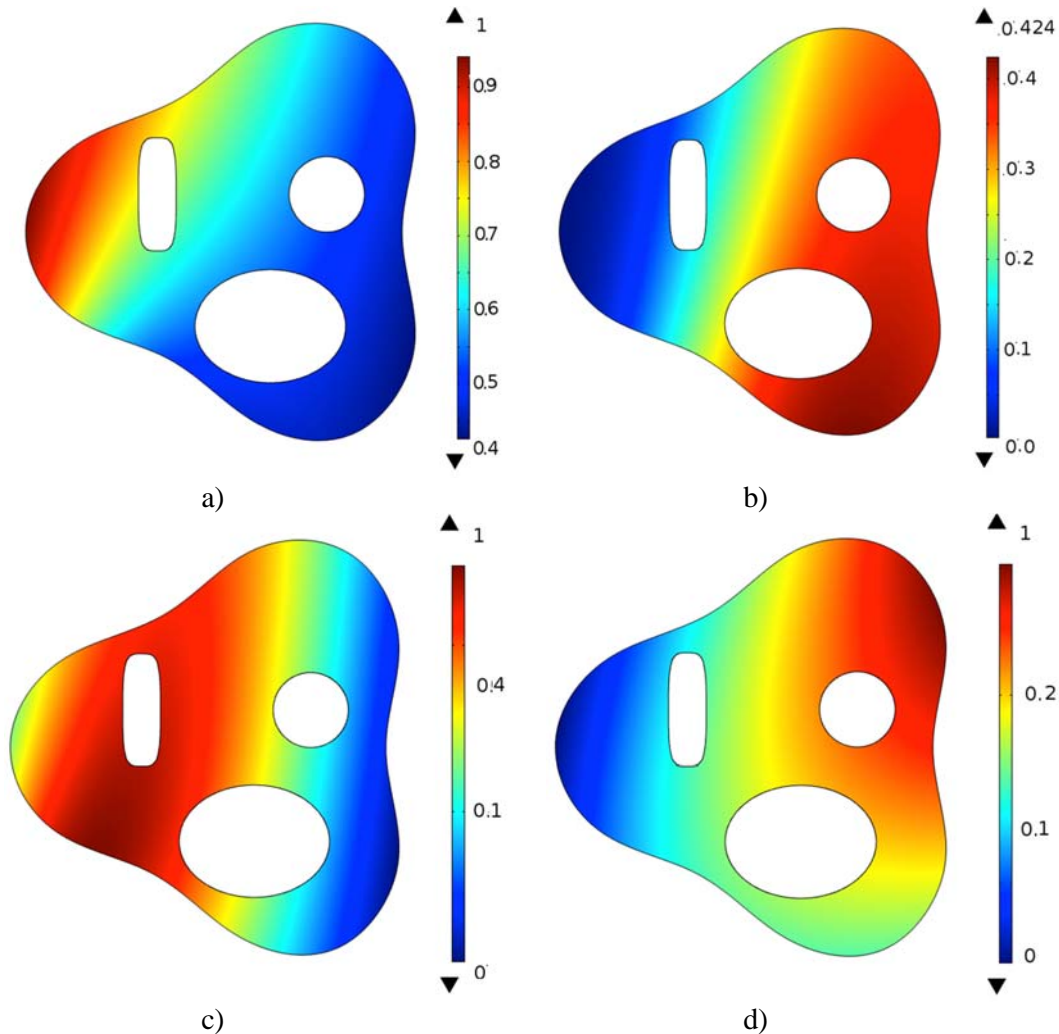


Figure 8. Case 3: Distribution of relative error in percents between exact thermal conductivity and converged conductivity with: a) 1% noise, b) 2% noise and c) 3% noise and d) relative error between exact heat capacity and converged heat capacity with 3% error

### CONCLUSIONS

The methodology for estimating parameters in analytic models for spatial distribution of thermal conductivity was extended to also estimate parameters in analytic models for spatial distribution of heat capacity within arbitrarily shaped multiply-connected 2D solid objects. The material property can be non-destructively estimated by minimizing the sum of normalized least squares between the calculated and measured boundary temperatures. The numerical integration of the governing elliptic partial differential equation for steady state temperature field was performed using the finite element method,

which was validated against an analytic solution. An efficient surrogate model in the form of a multi-dimensional response surface supported by the high fidelity finite element solutions was created to facilitate very fast approximate solutions of the analysis problem, thereby significantly reducing computing time for the minimization algorithm to converge. The inverse determination methodology showed promising results in being able to accurately determine linear and highly non-linear spatial distributions of these two thermal properties. This inverse parameter identification technique has also proven to be stable, thus, robust and accurate even when the boundary temperature measurements contained noise. This truly non-destructive methodology is also directly applicable to simultaneous determination of spatially varying mechanical properties and electrical properties. It is also straightforward to extend this method to arbitrarily shaped multiply-connected 3D objects and to apply it in inverse determination of time-varying material properties. The current drawback of the presented method is that it requires an *a priori* knowledge of the spatial analytic variations of the physical properties. This can be remedied by representing such variations using products of truncated series such as Fourier or Chebyshev and determining correct values of their coefficients. Future works can also include solving the inverse problem within the Bayesian framework to cope with the uncertainties and noise arising from measurements.

### ACKNOWLEDGEMENTS

The lead author gratefully acknowledges the financial support from Florida International University in the form of an FIU Presidential Fellowship. The authors are grateful for the research funding provided by the NSF research grant NSF CBET-1642253 monitored by Dr. Jose Lage. The views and conclusions contained herein are those of the authors and should not be interpreted as necessarily representing the official policies or endorsements, either expressed or implied, of NSF or the U.S. Government.

### REFERENCES

- [1] Chen, B., Chen, W., Cheng, H.D., Sun, L.-L., Wei, X. and Peng, H. [2016], Identification of the Thermal Conductivity Coefficients of 3D Anisotropic Media by the Singular Boundary Method. *International Journal of Heat & Mass Transfer*, Vol. 100, pp 24-33.
- [2] Gu, Y., Chen, W. and Fu, Z. [2014], Singular Boundary Method for Inverse Heat Conduction Problems in General Anisotropic Media, *Inverse Problems in Science and Eng.*, Vol. 22, No. 6, pp 889-909.
- [3] Fu, Z., Chen, W. and Zhang, C. [2012], Boundary Particle Method for Cauchy Inhomogeneous Potential Problems. *Inverse Problems in Science and Engineering*, Vol. 20, No. 2, pp 189-207.
- [4] Mohebbi, F. and Sellier, M. [2016], Estimation of Thermal Conductivity, Heat Transfer Coefficient, and Heat Flux Using a Three-Dimensional Inverse Analysis. *International J. of Thermal Science*, Vol. 99, pp 258-270.
- [5] Guo, Y., Shen, Y. and Tan, J. [2016], Stochastic Resonance in a Piecewise Nonlinear Model Driven by Multiplicative Non-Gaussian Noise and Additive White Noise. *Communications in Nonlinear Science and Numerical Simulation*, Vol. 38, pp 257-266.
- [6] J. Sylvester [1990], An Anisotropic Inverse Boundary Value Problem, *Comm. Pure Appl. Math*, Vol. 43, pp 201-232
- [7] Rodrigues, F.A., Orlande, H.R.B. and Dulikravich, G.S. [2004], Simultaneous Estimation of Spatially-Dependent Diffusion Coefficient and Source Term in Nonlinear 1D Diffusion Problem, *Math. Comput. Simulation*, Vol. 66, pp 409-424.
- [8] Dulikravich, G.S., Reddy, S.R., Colaco, M.J. and Orlande, H.R.B. [2015], Inverse Determination of Spatial Variation of Diffusion Coefficients in Arbitrary Objects Creating Desired Non-Isotropy of Field Variables, *Material Science & Technology 2015 Conference*, Columbus, OH, USA, October 4-8

- [9] Dulikravich, G.S., Reddy, S.R., Pasqualetto, M.A., Colaco, M.J., Orlande, H.R.B. and Coverston, J. [2016], Inverse Determination of Spatially Varying Material Coefficients in Solid Objects, *Journal of Inverse and Ill-Posed Problems*, March 2016, DOI: 10.1515/jiip-2015-0057
- [10] Reddy, S.R., Dulikravich, G.S. and Zeidi, S.M.J. [2017], Inverse Non-Destructive Estimation of Spatially Varying Material Properties in 3D Solid Objects, to appear in *International Journal of Thermal Sciences*.
- [11] Naveira-Cotta, C., Orlande, H.R.B. and Cotta, R. [2011], Combining Integral Transforms and Bayesian Inference in the Simultaneous Identification of Variable Thermal Conductivity and Thermal Capacity in Heterogeneous Media, *ASME J. of Heat Transfer*, Vol. 133, pp 111301–111311
- [12] modeFRONTIER, Software Package, [2014], Ver. 4.5.4, ESTECO, Trieste, Italy.
- [13] Colaço, M.J. and Dulikravich, G.S. [2011], A Survey of Basic Deterministic, Heuristic and Hybrid Methods for Single-Objective Optimization and Response Surface Generation, in: *Thermal Measurements and Inverse Techniques*, Taylor & Francis, New York, pp 355–405.
- [14] Sobol, I.M. [1967], Distribution of Points in a Cube and Approximate Evaluation of Integrals, *U.S.S.R. Comput. Maths. Math. Phys.*, Vol. 7, pp 86-112.
- [15] Adorio, E.P. [2005], *MVF - Multivariate Test Functions Library in C for Unconstrained Global Optimization*, <http://geocities.com/eadorio/mvf.pdf>
- [16] MATLAB and Statistics Toolbox Release 2012b, awgn function, The MathWorks, Inc., Natick, Massachusetts, USA.
- [17] <http://www.omega.com/Temperature/>, visited 29 August, 2016
- [18] Dulikravich, G.S., Martin, T.J., Dennis, B.H. and Foster, N.F. [1999], Multidisciplinary Hybrid Constrained GA Optimization, in *EUROGEN99-Evolutionary Algorithms in Eng. and Computer Science: Recent Advances and Industrial Appl.* (eds. K. Miettinen, M. M. Makela, P. Neittaanmaki and J. Periaux), John Wiley & Sons, Jyvaskyla, Finland, pp 233-259.
- [19] Dulikravich, G.S., Martin, T.J., Colaco, M.J. and Inclan, E.J. [2013], Automatic Switching Algorithms in Hybrid Single-Objective Optimizers. *FME Transactions*, Vol. 41, No. 3, pp 167-179.